frontiers in Soil Science

TYPE Original Research
PUBLISHED 20 May 2026
DOI 10.3389/fsoil.2026.1814788

OPEN ACCESS

EDITED BY
Paloma Campos,
Spanish National Research Council (CSIC), Spain

REVIEWED BY
Joaquim C.G. Esteves Da Silva,
University of Porto, Portugal
Anna De Marco,
University of Naples Federico II, Italy
Fernando Rocha,
University of Aveiro, Portugal

*CORRESPONDENCE
Otávio dos Anjos Leal
o.dos.anjos.leal@fz-juelich.de

RECEIVED 21 February 2026
REVISED 14 April 2026
ACCEPTED 16 April 2026
PUBLISHED 20 May 2026

CITATION
Dias SC, Leal OA, Passe JJ, Pongo FL, Oliveira JR, Burgueño LET, Fernandez MBG, Pinto MAB, Silva JB, Job MTP, Nunes MCM and Stumpf L (2026) Potentially toxic elements and their impact on minesoil biota: a pioneering chronosequence study at the Moatize coal mine in Mozambique. *Front. Soil Sci.* 6:1814788. doi: 10.3389/fsoil.2026.1814788

Potentially toxic elements and their impact on minesoil biota: a pioneering chronosequence study at the Moatize coal mine in Mozambique

Sérgio da Costa Dias[1], Otávio dos Anjos Leal[2*], José João Passe[3], Fernando Luís Pongo[3], Jakeline Rosa de Oliveira[1], Luís Eduardo Torma Burgueño[1], Maria Bertaso de Garcia Fernandez[1], Marilia Alves Brito Pinto[4], Juliana Brito da Silva[1], Marcel Thomas Pereira Job[1], Maria Candida Moitinho Nunes[1] and Lizete Stumpf[1]

[1]Soil and Water Management and Conservation Program (MACSA), Soil Department, Federal University of Pelotas (UFPel), Pelotas, RS, Brazil, [2]Institute of Bio and Geosciences - Agrosphere (IBG-3), Forschungszentrum Jülich GmbH, Jülich, Germany, [3]Faculty of Geosciences and Environment, Púnguè University, Tete, Mozambique, [4]Postgraduate Program in Agronomy, State University of Southwest Bahia, Vitória da Conquista, Brazil

This study is the first to investigate the relationship between potentially toxic elements (PTEs) and soil fauna abundance across a chronosequence of minesoils in Moatize coal mine, Mozambique. Soil samples were collected (0.00–0.10 m layer) across a chronosequence of minesoils afforested for 0.5, 1.4, 5.3, and 10.6 years. One adjacent unmined soil was sampled as reference. The samples were analyzed for bioavailable Cr, Pb, Cu, Zn, and Ba contents, and their ecological risk factor and potential ecological risk index were assessed. Soil organic carbon content in the form of fulvic acid (C-fulvic), humic acid (C-humic) and humin (C-humin) as well as soil macro- and mesofauna organisms were quantified. The ecological risk factor and index values indicated low levels of contamination, with individual risk factors ranked as Cr>Cu>Ba>Pb>Zn, regardless of restoration time. Nevertheless, principal component analysis revealed antagonist interactions between Ba, Cu and Zn contents and fauna recolonization in the minesoil. Soil fauna abundance remarkably increased over restoration time, especially Acari, Collembola and Hymenoptera organisms, reaching 642, 227, and 143 organisms, respectively, after 10.6 years. This was accompanied by increased C-humic and C-humin concentration. Nevertheless, Acari, Collembola and Hymenoptera abundance in the 10.6-year restored minesoil were still 84%, 91% and 68% lower, respectively, compared to the unmined soil. Elapsed 10.6-years of restoration, minesoil fauna abundance and diversity increased, but this process seems to be hindered by residual contamination of the minesoil with PTEs, mainly Cu, Zn, Ba, and Cr. Our data may serve as a baseline for long-term environmental monitoring, as well as guidelines for policymakers defining restorations strategies in Moatize. This is critical as legislative reference values of PTEs are not established in this region.

KEYWORDS

ecological risk, heavy metals, humic substances, macrofauna, mesofauna, PCA

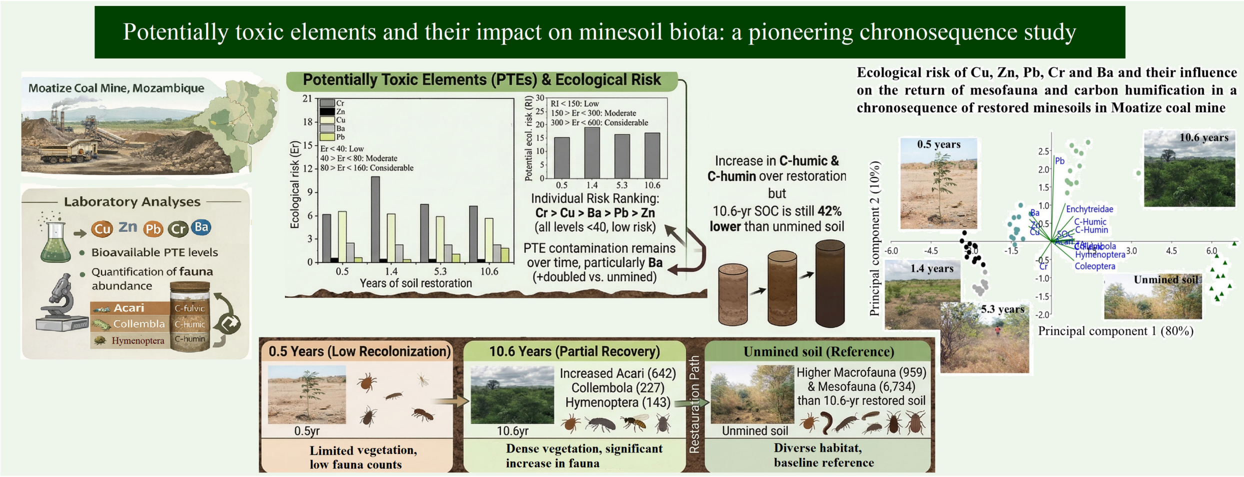

GRAPHICAL ABSTRACT

1 Introduction

Surface coal mining profoundly alters pedogenesis by removing native soil horizons and exposing geogenic materials with limited biological functionality, generating minesoils characterized by poor structural development, nutrient imbalance, and elevated concentrations of potentially toxic elements (PTEs) (1, 2). In these newly formed substrates, ecosystem recovery depends not only on vegetation establishment but also on the progressive restoration of biogeochemical processes controlling organic matter stabilization, nutrient cycling, and contaminant immobilization (1, 3). Because mine-derived materials frequently contain elevated content of trace metals inherited from overburden and coal residues, restoration of post-mining landscapes must be interpreted simultaneously as an ecological reconstruction process and a long-term soil pollution mitigation strategy (4, 5).

Mozambique hosts one of the largest coal reserves in Africa, with the Moatize coal basin recognized as one of the world's largest unexplored coal provinces (6). Surface coal extraction in this region generates large volumes of waste material that are commonly returned to open pits during landscape reconfiguration (7), forming overburden-derived minesoils. These substrates typically present severe physicochemical limitations for revegetation (8), including low nutrient availability, extreme pH values, high salinity, and elevated concentrations of PTEs such as Zn, Cu, Ni, Co, Pb, Cr, and Ba, all of which constrain biological establishment and early pedogenic development (9, 10).

Although chronosequence approaches have been widely applied to assess physicochemical recovery in reclaimed mine areas (11, 12), considerably less attention has been given to the interaction between bioavailable PTEs, soil organic matter humification, and biological recolonization under tropical conditions. This limitation is particularly relevant because soil biological communities are often more sensitive than conventional chemical indicators to early restoration constraints, especially where residual contamination persists (13, 14). Soil fauna directly contributes to litter fragmentation, aggregate formation (10), microbial habitat regulation, and nutrient cycling (15), making it a highly integrative indicator of whether technogenic substrates effectively transition toward biologically functional soils (16).

In the Moatize mining region, previous studies have primarily focused on contamination risks in surrounding water bodies and adjacent soils due to concerns related to human and animal exposure (17, 18). However, the internal ecological trajectory of reclaimed minesoils remains largely unexplored, particularly regarding the simultaneous evolution of PTE bioavailability, humified organic carbon fractions, and soil fauna abundance. This gap is especially relevant in tropical systems, where high temperature and seasonal rainfall may accelerate organic matter turnover, alter contaminant redistribution, and generate restoration pathways distinct from those reported in temperate mining environments.

Elevated concentrations of coal-derived PTEs may persist as long-term ecological stressors, influencing contaminant mobility, biological recolonization, and the overall trajectory of minesoil restoration (19, 20). Although the toxicity of these elements is well recognized, their effects on soil fauna recovery across tropical mine chronosequences remain insufficiently understood. Organic matter humification may play a decisive role in this process, particularly because stable humic fractions can reduce PTE mobility and biological exposure over time (21, 22), thereby contributing to contaminant buffering and ecological stabilization.

Increasing restoration age is expected to promote progressive reductions in the ecological risk associated with bioavailable PTEs, accompanied by greater accumulation of stable organic carbon fractions and increased soil fauna abundance (23). Humin-enriched fractions are also expected to be associated with lower biological exposure to trace elements, reflecting the gradual development of contaminant buffering mechanisms during ecosystem recovery (24, 25). Therefore, this study provides the first integrated assessment of bioavailable PTEs, humic substance fractions, and soil fauna recovery across a 10.6-year tropical coal minesoil chronosequence in Mozambique. By linking ecological risk indicators with biological and organic matter attributes, the study advances current understanding of how reclaimed minesoils evolve from chemically unstable mine substrates toward ecologically functional systems and establishes evidence-based benchmarks for restoration monitoring in tropical coal mining regions.

2 Materials and methods

2.1 Study area characterization

The study was conducted in Mozambique, Tete province, in the Moatize coal mining area (Figure 1). This region is characterized by a hot semi-arid climate in the Köppen-Geiger climate classification, as described by Peel et al. (26). About 71% of rainfall occurs in the summer months (December, January and February), when temperatures are highest (23.2 °C on average). The driest period of the year is from May to September, with monthly rainfall ranging from 2 to 5 mm (Figure 2).

The Moatize coal basin occupies approximately 137,000 km^2 in the Mozambican territory and the predominant geological formation consists of sandstones, siltstones and mudstones, deposited during the Carboniferous Period (17). Its geological framework comprises the Vúzi, Moatize, and Matinde formations, deposited from the late Carboniferous to Permian under evolving sedimentary environments, initially dominated by fan-delta and lacustrine-delta systems and later by braided fluvial channels and floodplains, reflecting tectonic reactivation and climatic oscillations. Coal seams exhibit cyclic alternations of coal and mudstone layers, indicative of fluctuating hydrological conditions during deposition, while the basin's thermal evolution was controlled mainly by burial processes with localized influence of Jurassic doleritic intrusions. Palynological evidence indicates that coal-bearing strata span from the middle to late Permian, consistent with Gondwanan depositional sequences and regional paleogeographic connectivity (27, 28). Open pit mining in Moatize produces about 11 million tons of coal annually (29). Once the coal extraction is completed, the topographic recomposition of the mined area starts. Over the mining overburden, which returns to the open pit, a 0.20 m layer of the A horizon of the original soil (previously removed and stored during coal extraction) is spread (Figure 3a). These activities are performed using specialized machinery, such as bulldozers, excavators and soil scrapers. Some more compacted sites are scarified to alleviate compaction and thereafter revegetation begins.

These minesoils are revegetated by the mining company by planting a mixture of native and exotic tree species adapted to the climatic and soil conditions of the area, mainly: *Libidibia ferrea*, *Afzelia quanzensis*, *Pterocarpus angolensis*, *Vachellia farnesiana*,

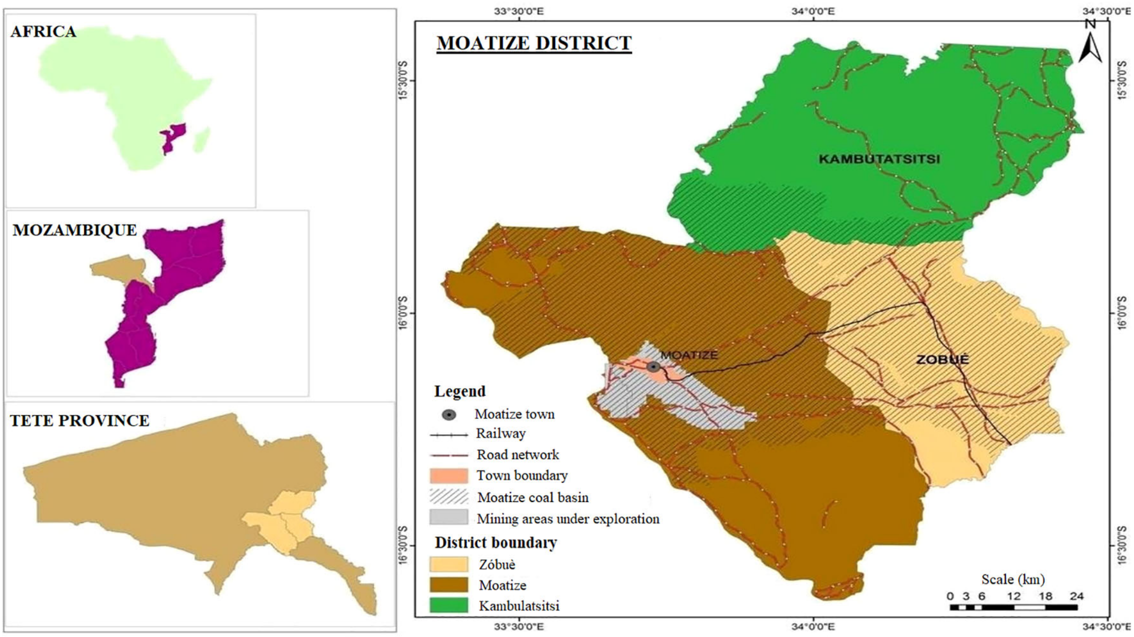

FIGURE 1
Geographic location of the study area in the Moatize coal-mining region, Tete Province, Mozambique.

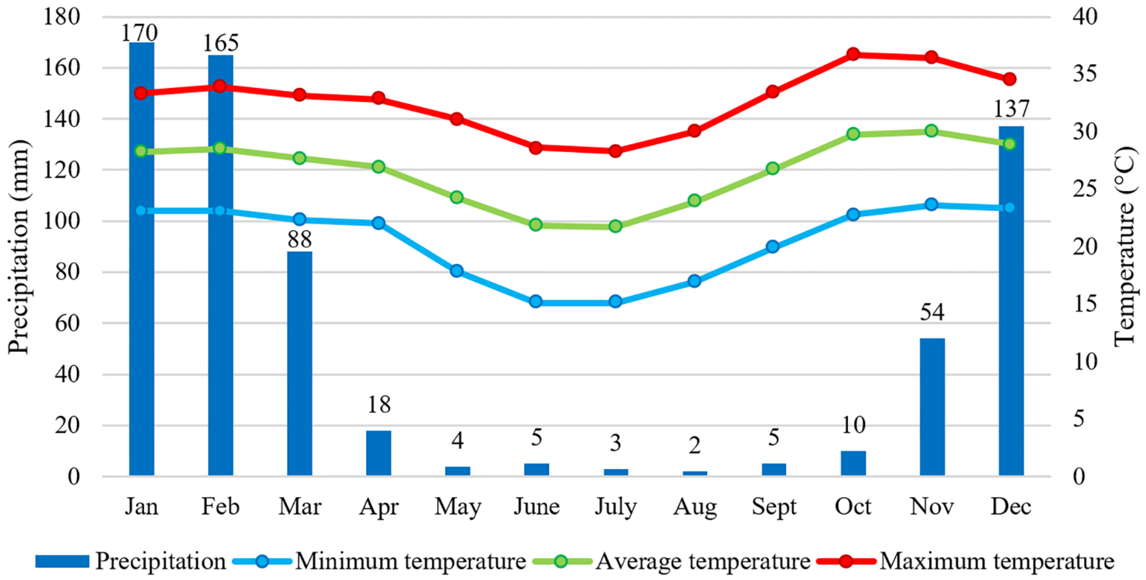

FIGURE 2
Monthly precipitation and temperatures, minimum, average and maximum, in the city of Moatize, Mozambique, from 2000 to 2023 (Adapted from INAM, 2023).

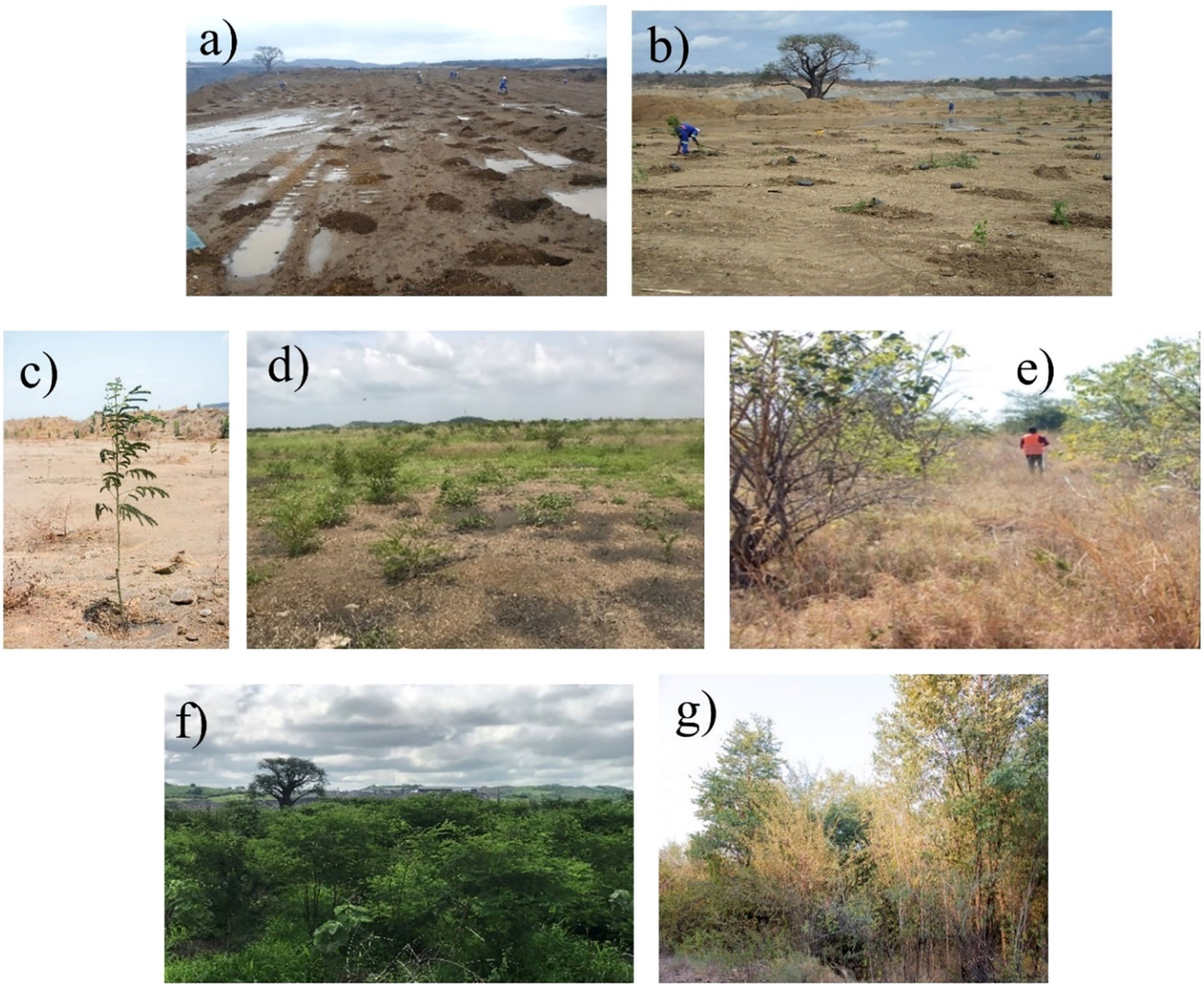

FIGURE 3
Minesoil at end of topographic recomposition **(a)**, start of minesoil revegetation **(b)**, minesoil revegetated for 0.5 **(c)**, 1.4 **(d)**, 5.3 **(e)** and 10.6 years **(f)** and unmined soil **(g)** in the Moatize coal mine region in Mozambique.

Dalbergia melanoxylon, *Combretum imberbe*, *Albizia quimmifera, Zizyphus mauritania*, *Colophospermum mopane*, *Mimusops coriacea*, *Brachystegia spiciformis* and *Adansonia digitate* (Figures 3b-f). Planting is carried out with approximately 30 seedlings of 10 different species per 10 m^2. Immediately after planting, dolomitic limestone and NPK chemical fertilizer (12–24–12) are applied to the soil. During the first and second year of restoration, these areas are managed by mulching with dry grass and at the end of the second year, top dressing is applied. The reference site (unmined soil) is covered mainly by the following species *Pterocarpus angolensis*, *Khaya anthotheca*, *Afzelia quanzensis*, *Acacia manguim*, *Eucalyptus globulus* and *Moringa oleifeira* (Figure 3g).

Regosols is the predominant soil type in the Moatize region, including the soil sampled as reference site (30).

2.2 Soil sampling and analyses

Soil sampling was conducted in 2023 in a chronosequence of minesoils with 0.5, 1.4, 5.3 and 10.6 years of restoration and in one unmined soil (reference). In each site, soil samples were collected at the 0.00–0.10 m layer in three 100 m transects, with 25 m intervals between each collection point, totaling 12 replicates per site. At each collection point, five soil sub-samples were gathered using a Dutch auger and thoroughly homogenized to form a composite sample. These samples were subsequently used for the analysis of PTEs, total soil organic carbon (SOC), and its chemical fractions (fulvic acid, humic acid, and humin). The physical and chemical characterization of the soils is presented in Table 1 as supplementary information for the discussion. The minesoils and unmined soil exhibited same textural class, allowing the reliable application of the chronosequence approach and the comparison of the minesoil attributes to that of the reference soil.

2.2.1 PTEs and ecological risk factor of individual PTEs and potential ecological risk index

The contents of bioavailable Cr, Pb, Cu, Zn, Mn and Ba in the soil samples were determined according to the acetic acid method of Ure (31), based on the EUR 19774 (BCR) protocol for bioavailable fractions (32). For that, 40 ml of acetic acid solution (0.11 mol L^{-1}) was added to 1 g of soil in a centrifuge tube. The tubes were shaken horizontally for 20 h. Thereafter, the samples were centrifuged for 15 minutes at 3000 rpm. The supernatant was transferred to a 50 ml container and the content of bioavailable Cr, Mn, Pb, Cu and Zn was determined by atomic absorption spectrometry. For Ba, flame photometry was used.

The individual ecological risk factor (Er) was obtained using Equation 1, which weighs the contamination level by its toxic potential and ecological sensitivity. Thus, Er reflects the potential ecological risk of each PTE individually. The Er of a given PTE was calculated according to Hakanson (33):

$$Er = Ti * CF \quad (1)$$

where: Er = ecological risk factor; Ti = toxic response factor for a given element (i.e., Pb = Cu = 5, Cr = 2, Zn = Ba =1) (23); CF = contamination factor (calculated by Equation 2), used to calculate the anthropogenic contribution to the contents found in the soil. The CF was calculated by dividing the content of a given element found in the soil by a background content of the same element (please see Equation 2). Here, the background contents of Pb, Cu, Cr, Zn, Ba, Mn were assumed as 25, 14, 42, 70 and 362 mg kg^{-1}, respectively. In this study, world background soil was obtained from the global averages reported by Kabata-Pendias (34). Specifically, values were extracted from the comprehensive dataset in Table 3.2 (column ‘a’, pages 41-42) of the aforementioned study.

$$CF = \frac{Content\ of\ each\ element}{Background\ content\ of\ each\ element} \quad (2)$$

The total potential ecological risk index (RI) was determined as the sum of individual ecological risk factors, representing the combined Er values of all investigated elements. The RI, originally proposed by Hakanson (33), quantitatively expresses the sensitivity of biological communities to the cumulative presence of potentially toxic elements (PTEs) in soil. Its applicability in coal mining environments has been supported by recent studies reporting significant ecological implications associated with PTE accumulation (35, 36). The RI is calculated according to Equation 3:

TABLE 1 **Physical and chemical attributes in the 0.00–0.10 m layer of minesoils and unmined soil in the Moatize coal mine region in Mozambique.**

Attributes	Minesoil restoration time (years)				Unmined soil
	0.5	1.4	5.3	10.6	
Clay (g kg^{-1})	276.33	277.50	279.67	272.00	274.33
Silt (g kg^{-1})	268.83	269.00	268.67	267.17	270.42
Sand (g kg^{-1})	454.83	453.50	451.67	460.83	455.25
Textural class	---- Sandy Clay Loam ---				
Bulk density (Mg m^{-3})	1.90	1.76	1.68	1.41	1.35
Macroporosity (m^3m^{-3})	0.07	0.10	0.14	0.15	0.18
Porosity (m^3m^{-3})	0.25	0.35	0.43	0.48	0.53
Soil pH in water	4.36	4.70	5.14	6.14	6.40
Base saturation (%)	30.50	66.36	70.33	91.04	97.32
Aluminum saturation (%)	10.03	2.06	1.34	0.37	0.38

$$RI = \sum Er = \sum (CF \star Ti) \quad (3)$$

where: RI (unitless) = potential ecological risk index computing all investigated PTEs, their contents and respective toxic response fator; Er is the single ecological risk index for a specific element (defined in Equation 1).

The interpretation of the results followed the classification proposed by Hakanson (33). For Er, values < 40 indicate low potential risk, 40–80 moderate risk, 80–160 considerable risk, 160–320 high risk, and > 320 very high risk. For RI, values < 150 correspond to low ecological risk, 150–300 moderate risk, 300–600 considerable risk, and > 600 very high risk. These classes allow for a comparison of the ecological relevance of different PTEs, as well as the overall threat level of the suite of contaminants in the study area.

2.2.2 SOC and chemical fractions

The Walkley-Black combustion method was employed to determine the SOC content (37). The soil organic matter fractionation was conducted according to Benites et al. (38), in which 20 mL of 0.1 mol L^{-1} NaOH was added to 1 g of soil to separate the extracts from humic and non-humic substances. After separating the aliquots, the extracts for determination of fulvic and humic acids were titrated with 0.0125 mol L^{-1} ammonium ferrous sulfate, while titration with 0.25 mol L^{-1} ammonium ferrous sulfate was performed for humin determination.

2.2.3 Soil fauna attributes

The Tropical Soil Biology and Fertility (TSBF) method was used for evaluation of soil macrofauna. A total of twelve soil monoliths were collected per area (0.20 m × 0.20 m x 0.10 m depth). All organisms visible to the naked eye were considered to belong to the macrofauna (39). The monoliths were transferred to the laboratory for sorting and collection of macrofauna organisms. During the field collection of monoliths, macrofauna organisms visible with naked eye on the monoliths were collected to prevent their eventual loss. The organisms collected in the field and laboratory were stored in bottles containing 70% alcohol for later identification.

Twelve steel cylinders (0.050 m heigh, 0.047 m diameter) were extracted from each area to quantify the soil mesofauna, invertebrates exhibiting Ø > 0.1 and < 2 mm. The mesofauna was extracted according to the Berlese-Tullgren funnel method. The soil samples were kept on 2 mm sieves in the extractor for 96 hours, exposed to light and heat of 25W lamps (temperature reached on the upper face of the cylinder was 42 °C). These conditions force the mesofauna organisms to move downwards out of the soil, where they are conducted through the funnel into collection bottles containing 30 ml of 70% alcohol.

The number of individuals of each taxon was counted and the various taxa were classified based on the number of individuals as follows: (1) Dominant: > 10% of the total number of individuals captured; (2) Common: 1–10% of the total number of individuals; (3) Rare: 0.1–1% of the total number of individuals; (4) Extremely rare: < 0.1% of the total number of individuals (40).

2.3 Statistical analysis

The effect of restoration time on PTEs, SOC, C-fulvic, C-humic and C-humin content was tested. Normality and homogeneity of variances were assessed using the Shapiro-Wilk test (S-W test) and analysis of variance (F test). When the difference between the restoration years was significant, linear and non-linear regression analyses were performed to discriminate the variation of the Time factor in each variable. The most representative models were adjusted to the data set and presented graphically and tabularly.

Simple linear regression analysis was used to describe the constant relationship between the predictor variable x (Time) and the response variables y (minesoil chemical and physical variables). Whenever the data presented different linear trends in different regions of the variables, segmented linear regressions (Piecewise regression and Linear Response Plateau - LRP) were tested. When the linear effect associated with the second line segment in the Piecewise regressions was not significant, the data set was fitted to an LRP-type regression model (41). The generic form of the simple linear regression equation with a single predictor variable can be expressed as in Equation 4:

$$y = \beta_0 + \beta_1 x + \varepsilon \quad (4)$$

where: y is the response variable; x is the predictor variable, β_1 are model parameters and ε is the random error.

Segmented linear regression applies linear regression to data (x, y) that do not have a linear relationship. That is, it introduces one or more inflection points, after which separate linear regressions are performed for the linear segments. Thus, the nonlinear relationship is approximated by linear segments (42). The Piecewise regression model can be developed in two or more straight line segments (Equations 5, 6), separated by inflection points (breakpoints - Bp). Each inflection delimits an abrupt change in the response function (y) of an influential variable factor (x). Bp can be interpreted as a critical, safe or limit value from which significant effects on the behavior of variables occur. In this study, a Piecewise regression model with two segments was use. d, which results in the two generic equations described below:

$$y = \kappa_1 + \beta_1 x, \ for\ x < x_{BP} \quad (5)$$

$$y = \kappa_2 + \beta_2 x, \ for\ x > x_{BP} \quad (6)$$

where: yr is the expected value of y for a given value of x; β_1 and β_2 are regression coefficients (indicating the slope of the line segments) and β_1 and β_2 are regression constants indicating the intercept points of the y-axis. The estimate of the value of yr, in the two regression segments fitted to the data, is given by the following expressions Equations 7 and 8:

$$y_r = region1\,(x) = [\beta_1(x_{Bp} - x) + \beta_2(x - x_1)]/(x_{Bp} - x_1) \quad (7)$$

$$y_r = region2(x) = [(\beta_2(x_2 - x) + \beta_3(x - x_{Bp})]/(x_2 - x_{Bp}) \quad (8)$$

where: d . e model parameters, x_{Bp} is the value of x at the breakpoint, x_1 and x_2, the minimum and maximum values of x, respectively.

Nonlinear regression of the LRP type (41) is also a segmented regression model, in two parts, in one of which the response variable is described by a simple linear regression model, and the other is described by a straight line parallel to the abscissa axis (plateau), where the response is constant (x_0). This model is described as follows in Equations 9 and 10:

$$y = \begin{cases} \beta_0 + \beta_1 x + \varepsilon, & x \le x_{Bp} \\ \beta_0 + \beta_1 x_{Bp} + \varepsilon, & x > x_{Bp} \end{cases} \qquad (9,\ 10)$$

where: y is the response variable (physical and chemical variables), β_0 and β_1 are, respectively, the intercept and slope of the line x is the level of the limiting input, ε is a random error term and x_Bp is the level of input required to reach the plateau. Thus, one can define.

(x_{Bp}, y_{Bp}), as the inflection point (breakpoint), at which the simple linear regression and plateau segments are inverted. The point at x of *Bp* for LRP regressions is given by the following expression Equation 11:

$$x_{Bp} = (\beta_2 - \beta_0)/\beta_1 \qquad (11)$$

The results of the various chemical and physical variables observed in the minesoil after 10.6 years of restoration were compared with observations made in the unmined soil, originating from an area of native vegetation. The difference between the variables in each of the environments was assessed using the Welch t-test. The normality of the data was verified using the S-W test. In the absence of normality or homogeneity of variances, comparisons were performed using the Mann-Whitney test and the homogeneity of variances was verified using the Brown-Forsythe test, respectively. In all analyses performed, the significance of differences was tested at the α=0.05 level. Data were processed in the statistical analysis program SigmaPlot V.15.

The impact of restoration years on the macrofauna and mesofauna of minesoils was discussed considering their total abundance, expressed as the total number of individuals per taxonomic group, the total number of individuals (summing all taxonomic groups), and their categorization into Dominant, Common, and Rare during the restoration periods in which minimal revegetation was established in the minesoils, i.e., between 1.4 and 10.6 years (Figures 3d-f). Finally, principal component analysis (PCA) was used to analyze the influence of restoration time and PTEs on soil fauna communities for the groups categorized as dominant. The PCA was performed using the software PAST 4.03.

3 Results

3.1 PTEs content along the minesoils chronosequence and unmined soil

Among the PTEs, Cu, Zn and Pb showed a linear behavior, while Cr and Ba were better explained by LRP regressions (Supplementary Table 1). The highest average levels of Cu and Zn were observed at the beginning of the restoration, at 0.5 years, with most samples above 90 and 30 mg kg^{-1}, respectively. However, both Cu and Zn decreased significantly over time, culminating in average contents of 80.14 and 27.26 mg kg^{-1} at 10.6 years of restoration (Figures 4a, b). At this stage of restoration, the Cu and Zn contents of the minesoil were still 98.5% and 50.61% higher than those of the unmined soil, respectively (Table 2). Unlike Cu and Zn, Pb content increased significantly throughout the chronosequence, especially between 5.3 and 10.6 years of restoration, when values increased from 25.92 to 45.48 mg kg^{-1} (Figure 4c). The Pb content in the oldest minesoil was 244% higher than in the unmined soil (Table 2).

For Cr, regression results revealed a significant increase until 1.4 years of restoration, from 52.44 to 93.25 mg kg^{-1}. However, from this period onwards there was a stabilization of Cr levels in the minesoils at around 60 mg kg^{-1} (Figure 4d). Compared to the unmined soil, the Cr content in the 10.6 years minesoil was 38.4% higher (Table 2).

According to the regression model, Ba levels decreased sharply between 0.5 years (878 mg kg^{-1}) and 1.4 years (809 mg kg^{-1}) of restoration and stabilized at around 800 mg kg^{-1} after this period (Figure 4e). As with the other PTEs, in the minesoil at 10.6 years of restoration, the Ba content was 98% higher than in the unmined soil (Table 2).

3.1.1 Ecological risk factor of individual PTEs and potential ecological risk index along the minesoils chronosequence

In general, the Er of the single PTE in the soil of the Moatize Mine, considering bioavailable levels, was generally low (Er < 40), and the RI for Cr, Zn, Cu, Ba and Pb indicated low ecological risk potential (RI < 150), regardless of restoration time (Figure 5). The potential risk indices of individual PTEs decreased as follows: Cr>Cu>Ba>Pb>Zn. Cr was the PTE with the highest Er value (11), followed by Cu (7), with small variations (<1) over the chronosequence (Figure 5).

Among the PTEs, Zn exhibited the lowest Er, despite having average concentrations of 30 mg kg^{-1} in the soil (Figure 4b), which is 2.3 times lower than the world average value of 70 mg kg^{-1} (24) and remained practically unchanged throughout the chronosequence. The RI, which considers the individual risks of Cr, Zn, Cu, Ba and Pb, indicates a low ecological risk in the regenerated area of the Moatize Mine. When looking at the RI in relation to the restoration time of the area, the highest RI of 20.4 was obtained at 1.4 years (Figure 5), with a contribution of 54.4% of Cr to this index.

3.2 SOC and chemical fractions along the minesoils chronosequence and unmined soil

The SOC, C-humic and C-humin content over restoration time was best fitted to a Piecewise model, while for C-fulvic content the best fit was a LRP model (Supplementary Table 2). For SOC, the first important moment of content increase occurred close to 2 years of restoration, although the contents were below 3 g kg^{-1}. The

10.3389/fsoil.2026.1814788

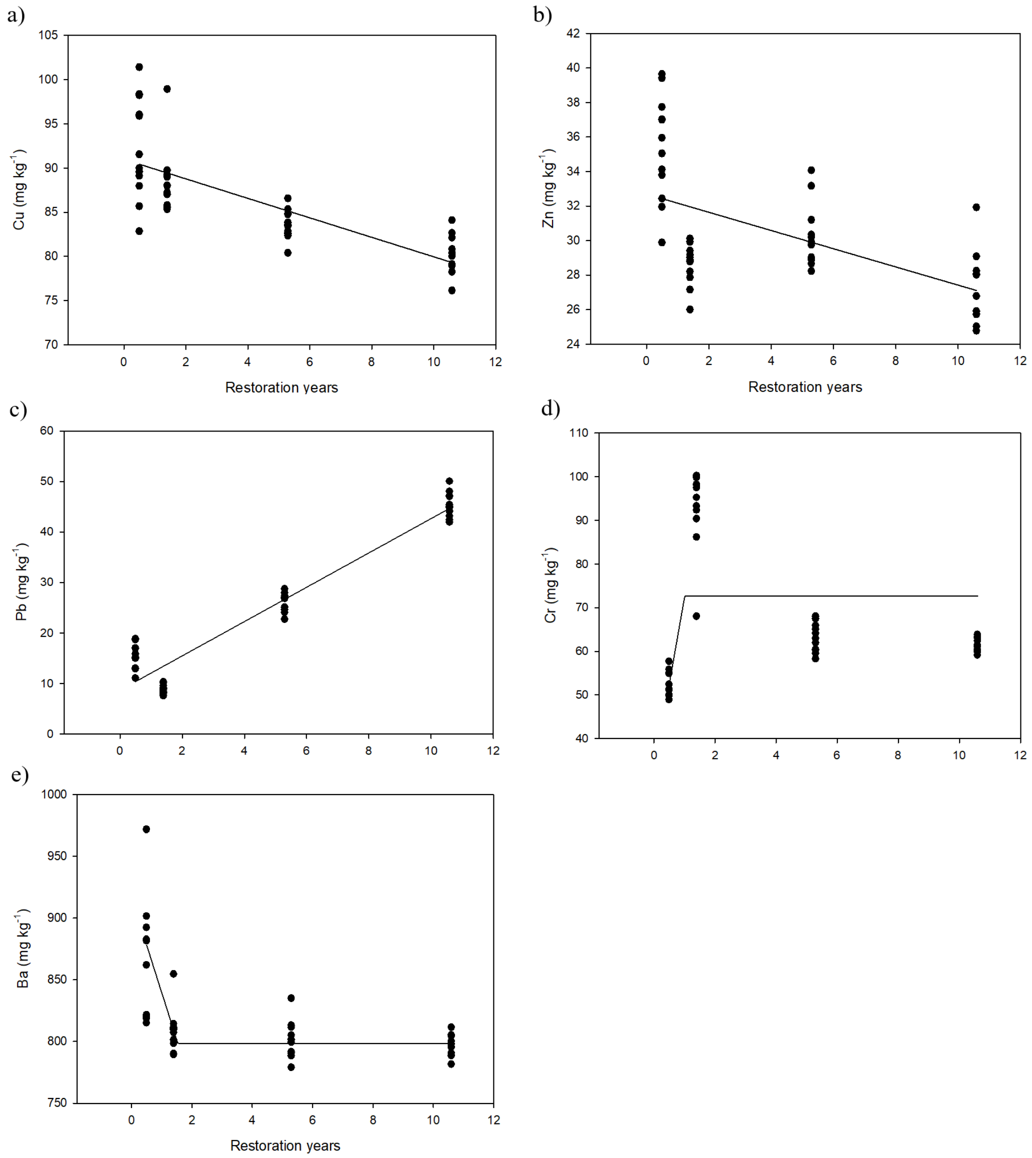

FIGURE 4
Regression model for Copper **(a)**, Zinc **(b)**, Lead **(c)**, Chromium **(d)** and Barium **(e)** in the 0.00-0.10 m layer along a chronosequence of minesoils in the Moatize coal mine region, Mozambique.

second moment of SOC increase occurred at 10.6 years when contents exceeded 6 g kg^{-1} (Figure 6a). Nevertheless, such SOC content was still significantly lower than that observed in the unmined soil (10.4 g kg^{-1}) (Table 2).

Soil C-fulvic content increased up to 5.3 years of restoration, followed by a stabilization at around 1.3 g kg^{-1} (Figure 6b). For C-humic content, a slight increase occurred until 5.3 years of restoration (0.11 g kg^{-1}), followed by a remarkable increase to 0.90 g kg^{-1} at 10.6 years of restoration (Figure 6c). The C-humin content increased with restoration time, mainly between 0.5 and 5.3 years, as indicated by the slope of the curve, reaching 2.38 g kg^{-1} at 10.6 years of restoration (Figure 6d). Overall, the C-fulvic, C-humic and C-humin contents were significantly higher in the unmined soil compared to the oldest minesoil (Table 2).

3.3 Soil fauna along the minesoils chronosequence and unmined soil

The unmined soil contained 959 macrofauna and 6,734 mesofauna individuals (Table 3). Contrastingly, the minesoils with 1.4, 5.3 and 10.6 years of restoration contained 24, 84 and 274 macrofauna individuals, respectively, which were distributed in 3, 4 and 6 taxonomic groups, of which Coleoptera and Hymenoptera were classified as dominant, and Araneae, Diplopoda, Diptera, and Hemiptera were classified as common (Table 3). For mesofauna, the number of individuals in the minesoil restored for 1.4, 5.3 and 10.6 years was 5, 193 and 893, respectively, which were distributed in 1, 4 and 4 taxonomic groups, with Acari, Collembola and Encytreideos standing out as dominant (Table 3).

TABLE 2 Differences between PTEs, SOC and chemical fractions of a minesoil with 10.6 years of restoration and the unmined soil in the Moatize coal mine.

Attributes	Soil use	Mean (n = 12)	Standard deviation	Brown-Forsythe test (*p*)	S-W test (*p*)	Welch test (*p*)
Cu (mg kg^{-1})	Minesoil 10.6 yrs	80.14	2.13	< 0.05	0.129	<0.001
	Unmined soil	53.21	3.62			
Zn (mg kg^{-1})	Minesoil 10.6 yrs	27.26	2.04	< 0.05	0.071	<0.001
	Unmined soil	13.74	0.85			
Pb (mg kg^{-1})	Minesoil 10.6 yrs	45.48	2.45	< 0.05	0.671	<0.001
	Unmined soil	13.22	0.78			
Cr (mg kg^{-1})	Minesoil 10.6 yrs	61.29	1.52	< 0.05	0.103	<0.001
	Unmined soil	44.29	8.29			
Ba (mg kg^{-1})	Minesoil 10.6 yrs	795.64	8.56	0.702	0.244	<0.001
	Unmined soil	401.69	8.22			
SOC (g kg^{-1})	Minesoil 10.6 yrs	6.04	0.85	0.492	0.144	<0.001
	Unmined soil	10.41	0.60			
C-fulvic (g kg^{-1})	Minesoil 10.6 yrs	6.04	0.02	0.492	0.144	<0.001 <0.001
	Unmined soil	10.41	0,32			
C-humic (g kg^{-1})	Minesoil 10.6 yrs	0.92	0.06	0.205	0.051	<0.001
	Unmined soil	1.12	0.06			
C-humin (g kg^{-1})	Minesoil 10.6 yrs	2.32	0.22	0.792	< 0.05	<0.001
	Unmined soil	4.20	0.21			

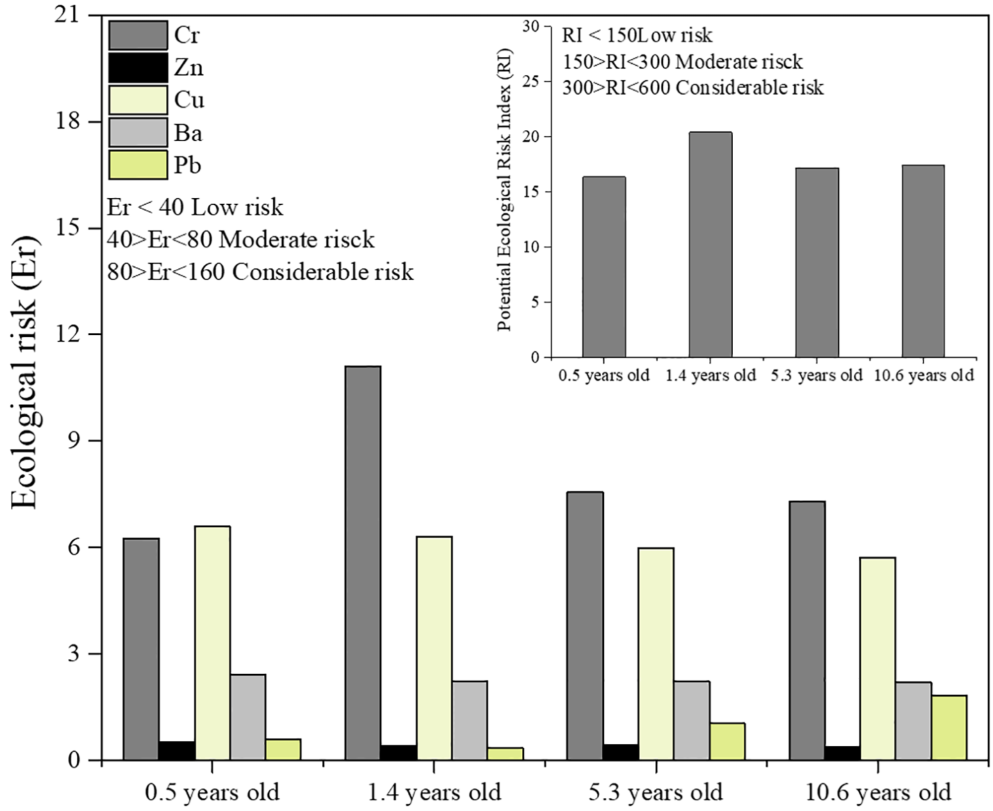

FIGURE 5
Potential ecological risk factor of individual PTEs (Er) and potential ecological risk Index (RI) of minesoils over a chronosequence of 10.6 years.

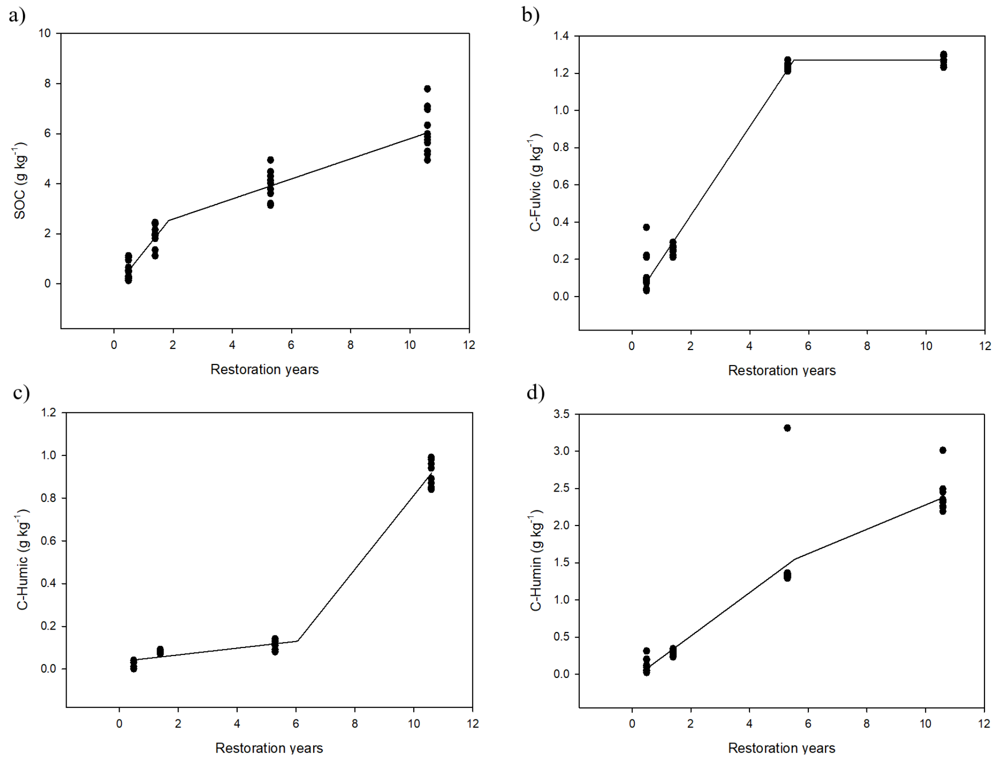

FIGURE 6
Regression model for SOC **(a)**, C-Fulvic **(b)**, C-Humic **(c)**, C-Humin **(d)** in the 0.00–0.10 m layer along a chronosequence of minesoils in the Moatize coal mine region, Mozambique.

TABLE 3 **Fauna groups and degree of dominance along the chronosequence of minesoils and unmined soil at the Moatize Mine in Mozambique.**

Soil fauna	Size	Restoration time (years)				Dominance degree[1]	
		1.4	5.3	10.6	Unmined soil	Minesoil	Unmined soil
Acari	Meso	0	124	642	3943	45.4***	58.7***
Araneae	Macro	0	9	13	153	5.2**	16.0***
Blattodea	Macro	0	0	0	19	0.0*	2.0*
Collembola	Meso	0	46	227	2434	16.4***	36.3***
Coleoptera	Macro	3	14	52	92	16.0***	9.6**
Diplopoda	Macro	0	0	16	86	1.9**	9.0**
Diplura	Meso	0	10	0	335	1.7**	5.0**
Diptera	Macro	0	8	37	70	7.7**	7.3**
Enchytraeidae	Meso	5	13	24	31	36.5***	0.5*
Hemiptera	Macro	3	11	13	62	10.0**	6.5**
Hymenoptera	Macro	18	42	143	446	59.1***	46.5***
Isopoda	Macro	0	0	0	31	0.0*	3.2**
Individual	Macro	24	84	274	959		
	Meso	5	193	893	6734		
Groups	Macro	3	5	6	8		
	Meso	1	4	4	4		

[1]Dominance degree: ***Dominant group (>10%); **Common group (1-10%); *Rare group (0.1–1%).

3.4 Principal component analysis

The first two components of PCA explained together 90% of total variance in the data (Figure 7). The first component (PC1) explained 80% while the second component (PC2) explained 10% of the variation. The right (positive) segment of PC1 displays closer relations between soil fauna organisms, SOC and SOC fractions eigenvectors mainly for the 10.6 years minesoil and the unmined soil (Figure 7). The opposite (negative) segment of PC1 displays the association of PTEs eigenvectors (Ba, Zn, Cu and Cr) with the youngest minesoils (0.5, 1.4 and 5.3 years). Noteworthily, the only PTE that was found in the positive portion of PC1 and PC2 was Pb, which was ordinated closely together with an increase fauna abundance in the 10.6-year minesoil (Figure 7). All the other PTEs showed antagonistic relationships with soil fauna organisms and with SOC and its fractions (Figure 7). The unmined soil was ordinated alone within a PCA quadrant (Figure 7), overall revealing that minesoil restoration is at initial stage even after 10.6 years.

4 Discussion

In general, Cu, Zn, and Ba contents were highest during the initial phase of restoration (Figure 4). Although their levels decreased over time, they remained significantly higher than those found in unmined soil (Table 2). For Cu, contents close to 100 mg kg^{-1}, which can be harmful to soil organisms (18), were found in the minesoils with up to 1.4 years of restoration (Figure 4a). Even after 10.6 years of restoration, the average Cu content was still 80.14 mg kg^{-1}, which is five-fold higher than that reported by Song et al. (43) in the 0.00–0.20 m layer of Chinese minesoils after seven years of restoration. Song et al. (43) also compared heavy metal concentrations in reclaimed minesoils and unmined soils, concluding that in unmined soils the metals originated from the parent material and were naturally more concentrated in deeper layers. In the Moatize minesoils this pattern differs, as the coal waste used in soil reconstruction has likely become the primary source of heavy metals in these minesoils. Nevertheless, the Er indicates a low risk for Cu (Er<40; Figure 5).

The Zn content was mostly elevated in the 0.5-year minesoil (30 to 40 mg kg^{-1} in individual replicates) (Figure 4b). However, these values found in the Moatize minesoils are considerably lower than those observed in minesoils by Ding et al. (44) in China (>200 mg kg^{-1}), which indicate an increased Er derived from atmospheric pollution by coal burning. The authors observed that Zn contents decreased significantly with increasing minesoil pH, as this affects Zn solubility. In the present study, Zn was the element that contributed least to Er (Figure 5). However, PCA results indicate that Zn strongly contributed to reduce soil fauna abundance (Figure 7). This deserves continued monitoring as Wierzbicka et al. (45) observed that the abundance of Acari organisms decreased along with the increase of Zn concentrations in Scots pine (*Pinus sylvestris L.*) residues entering the soil in Poland.

In relation to Ba, levels above 500 mg kg^{-1} in minesoils have been shown to inhibit the growth and reproduction of soil fauna organisms (18). In the Moatize minesoils, Ba contents remained above 750 mg kg^{-1}, regardless of restoration time (Figure 4e) and remained about 50% than that observed in the unmined soil even after 10.6 years of restoration (Table 2). These findings indicate that the topsoil added during the topographic restoration of the area was affected by the coal mining processes. According to Vasconcelos et al. (46), mining operations can release chemical elements naturally present in rocks, including Ba, which subsequently accumulate in the soil. The stabilization of Ba contents after 1.4 years of restoration (Figure 4e) may be attributed to Ba adsorption and precipitation in less soluble forms, such as Ba sulphates and carbonates (47). These reactions reduce Ba availability and its

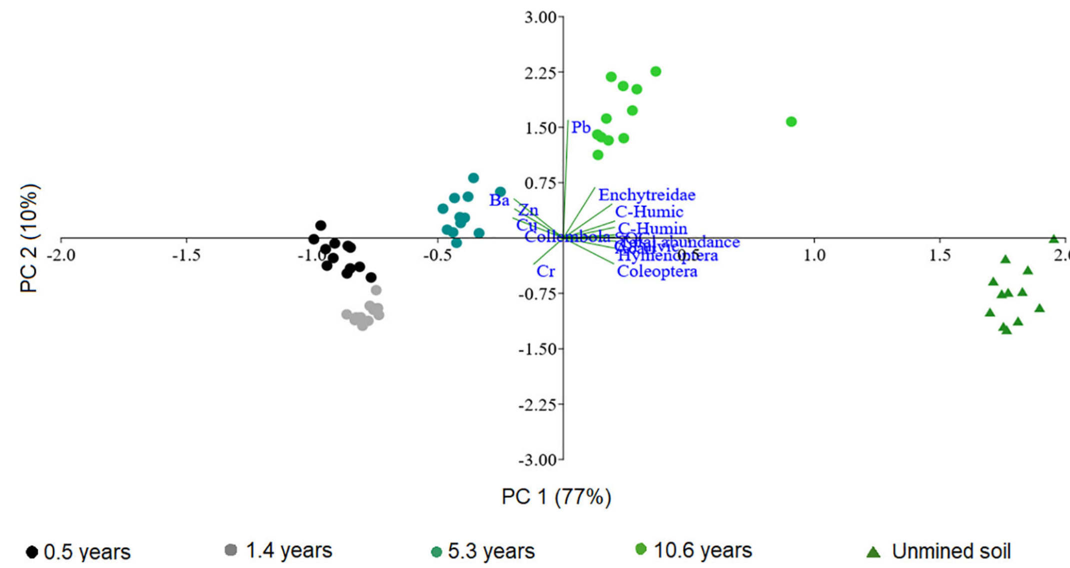

FIGURE 7
Principal component analysis of PTEs, soil fauna and SOC and its chemical fractions in the 0.00–0.10 m layer of minesoils and unmined soil in the Moatize coal mine region in Mozambique.

susceptibility to leaching, promoting its long-term retention in the soil (48). Although Ba offered a low Er (<40), it is worth noticing that after Cr, Ba was the element with the highest Er among the PTEs analyzed (Figure 5).

The temporal dynamics of Cr suggest a distinct geochemical behavior compared to Ba, likely influenced by the initial weathering of coal-derived minerals. The persistence of Cr levels above those found in unmined soils, even after a decade, underscores the role of the parent material (overburden and coal residues) as a continuous source of this element (49). This is consistent with the high Cr content typical of coal ash in the Moatize basin (46), which acts as a long-term reservoir. Although the Er for Cr remained in the low-risk category, its position as the most representative PTE in the total risk profile (RI) is concerning. This prominence is a direct reflection of Cr's intrinsic toxicity and environmental persistence (50). Studies show that less than 0.5% of total Cr is bioavailable in ultramafic mine spoils because Cr is mostly locked within insoluble silicate and oxide phases, limiting its mobility and environmental impact over short timescales (51). However, a portion of Cr can become mobilized over decades through slow weathering processes, potentially increasing bioavailability gradually (51). Chromium speciation strongly influences toxicity and bioavailability; trivalent Cr(III) tends to be immobile and less toxic, while hexavalent Cr(VI) is more soluble, mobile, and harmful but often present at low ratios in coal-related wastes (52, 53). Remediation strategies focus on reducing Cr(VI) to the less toxic Cr(III) form and stabilizing Cr in mineral phases to minimize environmental and health risks (52, 53). Our findings indicate that even if total concentrations do not reach critical thresholds, the cumulative nature of Cr in these technogenic substrates requires long-term monitoring to prevent potential bioaccumulation in the recovering trophic chain.

Particularly, Pb was the only PTE that increased in content over restoration time (Figure 4c). This trend may be related to increase in soil pH over time (Table 1), which is known to change the solubility and mobility of this metal (54). In the early stages of the chronosequence (0.5 and 1.4 years), soils were more acidic (Table 1), and under these conditions Pb mobilization and leaching may be facilitated. In contrast, increase in soil pH with restoration time (Table 1) may have decreased Pb solubility, favoring its adsorption to soil minerals and organic matter, leading to its gradual accumulation over time. This is in line with Pierangeli et al. (55), who observed that increase of soil pH from 4.5 to 6.5 increased Pb adsorption by up to 16.7 times. This is explained by the transition from monodentate to bidentate complexation reactions at higher pHs, which promotes Pb retention in the soil (56). Thus, the higher Pb contents in the Moatize minesoils compared to the unmined soil indicate that mining activity in the surrounding areas likely contributes to this result if considered that Vasconcelos et al. (46) found high Pb concentrations in coal ash generated in the Moatize sedimentary basin (74 mg kg^{-1}). Despite the increasing Pb content over restoration time, the Er of Pb was classified as low (<40) (Figure 5).

Overall, mining activities near the minesoils seem to contribute to the elevated contents of PTEs found in the minesoils compared to the unmined soil (Table 2). This contamination likely results from wind-transport and deposition of dust containing coal particles and PTEs (57), thereby contaminating the topsoil used in the future topographic restoration of the mined areas (58). In fact, it is common to observe the generation of intense dust at the Moatize mine, also because usually only few trucks are available to spread water to minimize this problem. In addition, excavation and removal of large volumes of soil and rock during mining can expose and release PTEs naturally present in geological layers, contributing to environmental contamination (57). Furthermore, coal combustion in thermal power plants, such as those operating at Moatize, also emits gases, particles, and ash containing PTEs. These PTEs can be transported through the air and deposited in the soil near the emission source (59). Coal ash, may contain high concentrations of PTEs, and if not properly retained by pollution control systems, can further contribute to soil contamination (58, 60).

The impacts of mining on soil fauna were more pronounced up to 5.6 years of restoration. In this period, the physical and chemical attributes of the minesoils were still inadequate (Table 1), which has been shown to negatively affect the return of soil organisms (61). However, a noticeable increase in the abundance of soil fauna organisms, especially those belonging to the Acari and Collembola groups, occurred between 5.3 and 10.6 years of restoration (Table 3). Together with the advancing establishment of the vegetation (Figure 3), this possibly stimulated the increase of SOC contents and its humic forms with restoration time (Figures 6a-d). The predominance of specific taxonomic groups at different stages of minesoil restoration reflects important shifts in community structure and dynamics over time, as well as their potential influence on the formation of different carbon fractions (62). As shown in Figure 6, the C-fulvic fraction, a most soluble and readily available form of carbon, increased up to 5.3 years of restoration and remained stable until 10.6 years. At 10.6 years, higher contents of C-humic and C-humin (Figures 6c, d) may be indicative of enhanced organic matter complexity (63). This coincided with a higher abundance of macrofauna organisms, suggesting its contribution to organic matter stabilization in association with improved soil structure (Table 1).

According to Sanghaw et al. (62) this shifts in fauna community and carbon complexity is a feedback process, while organic matter influences the structure and diversity of soil fauna, soil organisms, in turn, play a fundamental role in the dynamics of organic matter decomposition and stabilization. The marked increase in Acari and Collembola abundance between 5.3 and 10.6 years in Moatize aligns with findings by Frouz et al. (64), who demonstrated that microarthropods are the primary drivers of soil fabric development in post-mining chronosequences, transitioning from opportunistic colonization to stable community structures as the litter layer develops. Overall, microarthropods act as functional mediators that improve ecosystem recovery by fostering soil structure complexity and nutrient cycling during post-mining succession (64, 65). In the early stages of minesoil formation (1.4 years), a reduced fauna diversity was evidenced (Table 3), where predominant organisms are usually generalists and pioneers (Coleoptera, Hemiptera and Hymenoptera), capable of quickly colonizing environments still in under-optimal conditions (62). According to Chen et al. (66), these organisms play a crucial role in modifying and preparing the soil for future communities and are often adapted to extreme and challenging conditions. Over restoration time, new ecological niches are created, and fauna diversity increases. Between 5.3 and 10.6 years of restoration, mites and springtails were the taxonomic groups with the greatest increase in abundance (Table 3), and this possibly contributed to the increase in SOC, C-humic and C-humin content in the same period (Figure 6).

The increase in C-fulvic content up to 5.3 years reflects the rapid formation of labile organic matter, typical of early restoration stages, when fresh residues and easily degradable compounds predominate (67). This phase is marked by greater carbon mobility, contributing to nutrient cycling and initial soil restructuring (67, 68). This is coherent with the slight increase of C-humic content up to 5.3 years, followed by a marked rise, suggestive of intensified humification and formation of high-molecular-weight humic acids during intermediate succession stages (67, 69). This pattern, also observed in forest restoration areas, is associated with greater carbon stability and enhanced metal complexation in less bioavailable forms (70). Differently, C-humin increased steadily with restoration time, reflecting the gradual accumulation of recalcitrant organic matter fraction, as similarly reported for restored pastures and older post-mining soils (67, 70, 71). For instance, humin accumulation is an indicator of long-term carbon stability and sequestration (67–71). However, since the contents of all carbon fractions (C-fulvic, C-humic, and C-humin) remained significantly lower than in unmined soil (Table 2), it is plausible to consider that these minesoils are still at initial stage of functional restoration.

Overall, PTEs likely influenced the return of taxonomic groups throughout the studied chronosequence. Although low Er and RI values were observed (Figure 4), PCA revealed antagonistic relationships between the content of individual PTEs and the main faunal groups (Figure 7). Notably, higher Zn, Cu, Cr, and Ba contents observed at early restoration were negatively associated with fauna abundance. One possible explanation lies in the extraction method used for PTE determination. The use of acetic acid, a weak organic acid, primarily solubilizes the more mobile and exchangeable fractions in soil (31). This approach was selected over total concentration analysis because the bioavailable fraction provides a more sensitive and biologically relevant assessment of environmental risk for soil-dwelling organisms, as it excludes stable mineral phases that do not participate in immediate biochemical processes (72). While regulatory thresholds are typically based on total concentrations, several studies indicate that total levels are poor predictors of biological effects in complex technogenic substrates. Some studies have shown that the use of weak acid extractants, such as acetic acid, provides a better correlation with the metal content actually assimilated by soil invertebrates and plants (72–74), making it a superior proxy for assessing the success of soil remediation in mining areas. This methodological choice inevitably leads to lower Er and RI values compared to studies using total digestion. However, as demonstrated by Yu et al. (75) and Rincon-Vasquez et al. (76), the total concentration of a metal is a poor predictor of its ecotoxicity. By focusing on the labile fraction, we provide a more accurate representation of the chemical pressure exerted on the soil mesofauna and macrofauna. The 'low risk' classification (Er < 40) should therefore be interpreted as a measure of available toxicity, suggesting that even small fractions of mobile PTEs in these tropical minesoils are sufficient to significantly influence the biological recolonization process, as evidenced by our multivariate analysis.

The PCA also revealed a weak correlation between Pb contents and soil fauna abundance (Figure 7). This may be related to the predominant chemical forms of Pb in the minesoil, which can include Pb^{2+}; or complexes with carbonate ($PbCO_3$), hydroxide ($Pb(OH)_2$), or acetate ($(CH_3COO)_2Pb$), with their prevalence strongly influenced by soil pH (63). Thus, soil pH may have affected the bioavailability of Pb by altering its speciation or by directly influencing faunal establishment (77). In the older minesoils, where fauna abundance was higher, soil pH was slightly more alkaline (~6.5) compared to younger sites (0.5 and 1.4 years) (Table 1). Under these conditions, Pb likely occurred in less toxic forms, reducing or eliminating its adverse effects on soil fauna at the observed concentrations (Figure 4).

It should be noted that Mozambique currently lacks legislative references for Zn, Cu, Cr, Ba, and Pb contents to guide the assessment of PTE levels at the Moatize Mine. To fill this gap, a review of global literature was used as reference for Er assessment in our work. However, while this approach provides an initial basis for discussing the results, it is recognized that the conditions under which soil profiles were constructed after coal mining in Moatize may differ from those reported in the literature. This possibly explains the apparent contradiction between the low potential ecological risk values estimated for PTEs (Figure 5) and the negative correlation observed between these elements and the soil fauna in the minesoils (Figure 7).

Finally, the interaction between organic carbon fractions and PTEs is a key factor controlling metal bioavailability in minesoils. Humic and fulvic acids contain numerous negatively charged carboxylic and phenolic/hydroxyl groups that form stable complexes with metal cations, reducing their free fraction and, in many cases, their bioavailability and toxicity (78). The observed pattern, an initial increase in C-fulvic followed by a marked rise in C-humic and C-humin, suggests that, as restoration progresses, the soil develops more complexation sites and organo-mineral complexes. This process gradually decreases the exchangeable metal fraction, lowering its toxic potential for plants and soil organisms, which is essential for complex fauna community development.

5 Conclusions

This study investigated the impact of potentially toxic elements (Cu, Zn, Pb, Cr and Ba) on soil biota in minesoils across a 10.6-year restoration chronosequence. We found that the oldest restored minesoil (10.6 years) exhibits increased abundance and diversity of fauna taxonomic groups. However, macro- and mesofauna counts (274 and 893 individuals, respectively) remained far below those in unmined soil (959 and 6,734), which together with the slow vegetation establishment, likely restricted organic carbon accumulation, explaining a soil organic carbon content still 42% lower than the unmined soil.

The minesoil contamination with PTEs (mainly Cu, Zn, Ba, and Cr) likely impaired the return of fauna organisms to the minesoil.

For instance, Ba content at the oldest site was nearly double that in the unmined soil. The absence of legislative reference values poses a substantial challenge in evaluating the contamination and restoration of Moatize minesoils. Although low ecological risk indices were obtained for the evaluated elements, principal component analysis revealed a clear negative influence of these metals on the minesoil fauna abundance. With this study, we provide quantitative evidence to contribute to pollutant monitoring and the recovery of soil biodiversity in Mozambique.

Future research should focus on establishing site-specific ecotoxicological 'threshold values' for the Moatize district, using native soil organisms as bioindicators in controlled bioassays. Additionally, long-term monitoring (beyond the 10-year mark) is crucial to verify if the increasing humification of organic matter will effectively transition from a transient buffering state to a permanent immobilization of PTEs. Investigating the role of specific plant-microbe-fauna interactions in the rhizosphere could also reveal more assertive strategies to accelerate the conversion of these unstable mine wastes into functional tropical ecosystems.

Data availability statement

The original contributions presented in the study are included in the article/Supplementary Material. Further inquiries can be directed to the corresponding author.

Author contributions

SD: Conceptualization, Writing – original draft, Writing – review & editing, Project administration, Formal analysis, Methodology, Data curation. OL: Writing – review & editing, Investigation, Visualization. JP: Writing – review & editing, Formal analysis. FP: Formal analysis, Writing – review & editing. JO: Investigation, Funding acquisition, Writing – review & editing, Data curation, Resources. LB: Writing – review & editing, Formal analysis. MF: Writing – review & editing, Formal analysis. MP: Visualization, Validation, Methodology, Writing – review & editing. JS: Formal analysis, Writing – review & editing, Methodology, Data curation. MJ: Investigation, Writing – review & editing. MN: Writing – review & editing, Investigation. LS: Resources, Data curation, Writing – review & editing, Investigation, Funding acquisition.

Funding

The author(s) declared that financial support was received for this work and/or its publication. The authors thank CAPES and CNPq for financial support allowing the realization of this work. Dr. Stumpf thanks CNPq for the granted scholarship of first author (Process No. 305512/2025-0).

Acknowledgments

The authors thank Vulcan Mozambique, SA, for providing access to the study area as well as for the technical and logistical support provided. The first author expresses his gratitude to the Postgraduate Program in Soil and Water Management and Conservation Program of the Agronomy Faculty Eliseu Maciel – Federal University of Pelotas, Brazil. The authors thank the Companhia Riograndense de Mineração for logistical assistance. Generative AI (OpenAI, ChatGPT 5.3) was used only to partially elaborate the graphical abstract.

Conflict of interest

Author OA was employed by Forschungszentrum Jülich GmbH.

The remaining author(s) declared that this work was conducted in the absence of any commercial or financial relationships that could be construed as a potential conflict of interest.

Generative AI statement

The author(s) declared that generative AI was used in the creation of this manuscript. ChatGPT 5.3 (Open AI) was used to generate parts of the graphical abstract.

Any alternative text (alt text) provided alongside figures in this article has been generated by Frontiers with the support of artificial intelligence and reasonable efforts have been made to ensure accuracy, including review by the authors wherever possible. If you identify any issues, please contact us.

Publisher's note

Supplementary material

The Supplementary Material for this article can be found online at: https://www.frontiersin.org/articles/10.3389/fsoil.2026.1814788/full#supplementary-material

References

1. Gunathunga SU, Gagen EJ, Evans PN, Erskine PD, Southam G. Anthropedogenesis in coal mine overburden; the need for a comprehensive, fundamental biogeochemical approach. *Sci Total Environ*. (2023) 892:164515. doi: 10.1016/j.scitotenv.2023.164515

2. Spasić M, Borůvka L, Vacek O, Drábek O, Tejnecký V. Pedogenesis problems on reclaimed coal mining sites. *Soil Water Res*. (2021) 16:137–50. doi: 10.17221/163/2020-SWR

3. Feng Y, Wang J, Bai Z, Reading L. Effects of surface coal mining and land reclamation on soil properties: a review. *Earth Sci Rev*. (2019) 191:12–25. doi: 10.1016/j.earscirev.2019.02.015

4. Kracmarova-Farren M, Papik J, Uhlik O, Freeman J, Foster A, Leewis MC. Compost, plants and endophytes versus metal contamination: choice of a restoration strategy steers the microbiome in polymetallic mine waste. *Environ Microbiome*. (2023) 18:74–. doi: 10.1186/s40793-023-00528-3

5. Li Q, Yuan C, Wu Q, Peng Y, Zhao Z, Wang Y. Effects of vegetation restoration on the concentrations of multiple metal elements in post-mining soils. *J Environ Manage*. (2023) 347:119148. doi: 10.1016/j.jenvman.2023.119148

6. José DS, Sampaio CH. "State of the art of mining in Mozambique: Moatize coal case, Tete". In: *Proceedings of the 6° Luso-Mozambican Congress of Engineering (CLME'2011)* (Maputo, Moçambique: INEGI Editor). (2012). Available online at: https://www.ufrgs.br/rede-carvao/Sess%C3%B5es_A7_A8_A9/A9_ARTIGO_03.pdf (Accessed February 01, 2026).

7. Ramani RV. Surface mining technology: progress and prospects. *Proc Eng*. (2012) 46:9–21. doi: 10.1016/j.proeng.2012.09.440

8. Choudhury A, Lahkar J, Saikia BK, Singh AKA, Chikkaputtaiah C, Boruah HPD. Strategies to address coal mine-created environmental issues and their feasibility study on northeastern coalfields of Assam, India: a review. *Environ Dev Sustain*. (2020) 23:9667–709. doi: 10.1007/s10668-020-01091-4

9. Peplinski B, Czubak W. The influence of opencast lignite mining dehydration on plant production: a methodological study. *Energies*. (2021) 14:1917. doi: 10.3390/en14071917

10. Wang Y, Bai D, Zhang Y, et al. The role of afforestation with diverse woody species in enhancing and restructuring the soil microenvironment in polymetallic coal gangue dumps. *Environ Sci pollut Res*. (2024) 31:29916–29. doi: 10.1007/s11356-024-33164-6

11. Fernandez MBDG, Stumpf L, Miguel P, Pinto LFS, Carlos FS, Schubert RN, et al. Biological quality and organic matter dynamics in minesoil at 18 years reclamation with perennial grasses. *Ecol Eng*. (2023) 187:106866. doi: 10.1016/J.ECOLENG.2022.106866

12. Fernandez MG, dos Anjos Leal O, Oliveira Islabão G, Pagani Junior A, Vaz de Melo T, Knapp AP, et al. Temporal dynamics of minesoil restoration in Southern Brazil: A two-decade monitoring of soil physical attributes and organic carbon content. *Soil Tillage Res*. (2025) 253:106647. doi: 10.1016/J.STILL.2025.106647

13. Li X, Meng D, Li J, Yin H, Liu H, Liu X, et al. Response of soil microbial communities and microbial interactions to long-term heavy metal contamination. *Environ pollut*. (2017) 231:908–17. doi: 10.1016/j.envpol.2017.08.057

14. Shen Q, Fu W, Chen B, Zhang X, Xing S, Ji C, et al. Community response of soil microorganisms to combined contamination of polycyclic aromatic hydrocarbons and potentially toxic elements in a typical coking plant. *Front Microbiol*. (2023) 14:1143742. doi: 10.3389/fmicb.2023.1143742

15. Li J, Li Z, Sun Y, Lu J, Zhang Q, He X, et al. Succession characteristics and assembly process of soil microbiome at reclaimed farmlands in coal mining area. *Front Microbiol*. (2025) 16:1633687. doi: 10.3389/fmicb.2025.1633687

16. Kumar S, Singh AK, Ghosh P. Distribution of soil organic carbon and glomalin related soil protein in reclaimed coal mine-land chronosequence under tropical condition. *Sci Total Environ*. (2018) 625:1341–50. doi: 10.1016/j.scitotenv.2018.01.061

17. Bata EJ, Barreira CMCA, Almeida MG. Impacts socio-spatial and political-economic of mining megaprojects in Mozambique: the case of exploitation of the Moatize mineral coal. *Field-territory: Agrarian Geogr Magazine (Brazilian Journal)*. (2016) 11:93–122. doi: 10.14393/RCT112204

18. Alloway BJ. *Heavy Metals in Soils, Environmental Pollution*. Dordrecht: Springer Netherlands (2013). doi: 10.1007/978-94-007-4470-7

19. Mishra A, Lal B. Fate of potentially toxic elements derived from coal mining in soil. *Water Air Soil pollut*. (2024) 235:298. doi: 10.1007/s11270-024-07116-2

20. Tan M, Dong J, Qu J, Hao M. The patterns of migration of potentially toxic elements from coal mining subsidence areas and associated soils to waterlogged areas. *Toxics*. (2023) 11:888. doi: 10.3390/toxics11110888

21. de Souza ES, Dias YN, da Costa HSC, Pinto DA, de Oliveira DM, de Souza Falção NP, et al. Organic residues and biochar to immobilize potentially toxic elements in soil from a gold mine in the Amazon. *Ecotoxicol Environ Saf*. (2019) 169:425–34. doi: 10.1016/j.ecoenv.2018.11.032

22. Visconti D, Álvarez-Robles MJ, Fiorentino N, Fagnano M, Clemente R. Use of Brassica juncea and Dactylis glomerata for the phytostabilization of mine soils amended with compost or biochar. *Chemosphere*. (2020) 260:127661. doi: 10.1016/j.chemosphere.2020.127661

23. Xu C, Kuang S, He L, Wang C, Zu Y. Effects of changing restoration years on soil nutrient traits and plant community diversity in a phosphate mining area. *Forests*. (2023) 14:1468. doi: 10.3390/f14071468

24. Cui D, Kang Y, Xi B, Yuan Y, Liu Q, Tan W. Compost-enhanced humification of organic pollutants: mechanisms, challenges, and opportunities. *Environ Sci Ecotechnol*. (2025) 26:100575. doi: 10.1016/j.ese.2025.100575

25. Mosa A, Taha AA, Elsaeid M. In-situ and ex-situ remediation of potentially toxic elements by humic acid extracted from different feedstocks: experimental observations on a contaminated soil subjected to long-term irrigation with sewage effluents. *Environ Technol Innov*. (2021) 23:101599. doi: 10.1016/j.eti.2021.101599

26. Peel MC, Finlayson BL, McMahon TA. Updated world map of the Köppen-Geiger climate classification. *Hydrol Earth Syst Sci*. (2007) 11:1633–44. doi: 10.5194/hess-11-1633-2007

27. Bicca MM, Philipp RP, Jelinek AR, Ketzer JMM, dos Santos Scherer CM, Jamal DL, et al. Permian-Early Triassic tectonics and stratigraphy of the Karoo Supergroup in northwestern Mozambique. *J Afr Earth Sci*. (2017) 130:8–27. doi: 10.1016/j.jafrearsci.2017.03.003

28. Fernandes P, Hancox PJ, Mendes M, Pereira Z, Lopes G, Marques J, et al. The age and depositional environments of the lower Karoo Moatize Coalfield of Mozambique: insights into the postglacial history of central Gondwana. *Palaeoworld*. (2024) 33:979–96. doi: 10.1016/j.palwor.2023.07.001

29. Cuambe ISS. "Analysis of socio-environmental dynamics in mining areas: a study of coal exploration in Moatize-tete-Mozambique". In: *University of Vale do Paraíba*. Master's thesis. Brazil: University of Vale do Paraíba, São José dos Campos. (2016). Available online at: https://www.oasisbr.ibict.br/vufind/Record/BRCRIS_2a7b61f7c906139709ae87e9c2528672 (Accessed February 12, 2026).

30. Passe JJ. Indústria carbonífera no distrito de Moatize, província de Tete, Moçambique e sua influência ambiental dos solos por elementos potencialmente tóxicos (2018). Available online at: https://bdtd.ibict.br/vufind/Record/USP_91ba9d1f334237997bc20f9d96b5820b. Doctoral thesis, Federal University of São Paulo (Accessed February 12, 2026).

31. Ure AM. Single extraction schemes for soil analysis and related applications. *Sci Total Environ*. (1996) 178:3–10. doi: 10.1016/0048-9697(95)04791-3

32. Rauret G, López-Sánchez JF, Sahuquillo A, Rubio R, Davidson C, Ure A, et al. Improvement of the BCR three step sequential extraction procedure prior to the certification of new sediment and soil reference materials. *J Environ Monit*. (1999) 1:57–61. doi: 10.1039/a807854h

33. Hakanson L. An ecological risk index for aquatic pollution control a sedimentological approach. *Water Res*. (1980) 14:975–1001. doi: 10.1016/0043-1354(80)90143-8

34. Kabata-Pendias A. *Trace Elements in Soils and Plants*. Boca Raton, FL: Taylor & Francis (2011) p. 1–505.

35. Wu J, Zhu Q, Qiao N, Wang Z, Sha W, Luo K, et al. Ecological risk assessment of coal mine area based on "source-sink" landscape theory – a case study of Pingshuo mining area. *J Clean Prod*. (2021) 295:126371. doi: 10.1016/j.jclepro.2021.126371

36. Zerizghi T, Guo Q, Tian L, Wei R, Zhao C. An integrated approach to quantify ecological and human health risks of soil heavy metal contamination around coal mining area. *Sci Total Environ*. (2022) 814:152653. doi: 10.1016/j.scitotenv.2021.152653

37. Teixeira PC, Donagemma GK, Fontana A, Teixeira WG. *Manual de Métodos de Análise de Solos. 3ª edição Revista e Ampliada*. Brasília: Embrapa (2017). p. 573.

38. Benites VM, Madari B, MaChado PLOA. Extração e fracionamento quantitativo de substâncias húmicas do solo: um procedimento simplificado de baixo custo. In: *Comunicado Técnico Embrapa*, vol. 16. Rio de Janeiro: Embrapa Solos (2003). p. 7.

39. Lavelle P, Spain A, Blouin M, Brown G, Decaëns T, Grimaldi M, et al. Ecosystem engineers in a selforganized soil: a review of concepts and future research questions. *Soil Sci*. (2016) 181:91–109. doi: 10.1097/SS.0000000000000155

40. González G, Seastedt TR. Comparison of the abundance and comparison of litter fauna in tropical and subalpine forests. *Pedobiologia*. (2000) 44:545–55. doi: 10.1078/S0031-4056(04)70070-0

41. Oosterbaan RJ. Types of segmented regression and their statistical determination (2021). Available online at: https://www.waterlog.info (Accessed February 12, 2026).

42. Oosterbaan RJ. "Frequency and regression analysis". In: *Part II: Regression Analysis, Chapter 6. Drainage Principles and Applications, Publication* Wageningen, The Netherland: ILRI. (1994). 16:175–224.

43. Song W, Xu R, Li X, Min X, Zhang J, Zhang H, et al. Soil reconstruction and heavy metal pollution risk in reclaimed cultivated land with coal gangue filling in mining areas. *CATENA*. (2023) 228:107147. doi: 10.1016/J.CATENA.2023.107147

44. Ding YZ, Song ZG, Feng RW, Guo JK. Interaction of organic acids and pH on multi-heavy metal extraction from alkaline and acid mine soils. *Int J Environ Sci Technol*. (2014) 11:33–42. doi: 10.1007/s13762-013-0433-7

45. Wierzbicka A, Dyderski MK, Kamzcyc J, Rączka G, Jagodziński AM. Responses of soil mite communities (Acari: Oribatida, Mesostigmata) to elemental composition of

mosses and pine needles and long-term air pollution in Scots pine (Pinus sylvestris L.) stands. *Sci Total Environ*. (2019) 691:284–95. doi: 10.1016/j.scitotenv.2019.07.138

46. Vasconcelos L, Muchangos A, Siquela E. Elementos-traço em cinzas de carvões aflorantes de Moçambique. In: *Geochimica Brasiliensis (Brazilian Journal)*. Rio de Janeiro, RJ: Sociedade Brasileira de Geoquímica (2009) 23:344–61. Available online at: https://geobrasiliensis.org.br/geobrasiliensis/article/view/315 (Accessed February 08, 2026).

47. Cappuyns V. Barium (Ba) leaching from soils and certified reference materials. *Appl Geochem*. (2018) 88:68–84. doi: 10.1016/j.apgeochem.2017.05.002

48. Wang S, Li X, Qin Q. Study on surrounding rock control and support stability of ultra-large height mining face. *Energies*. (2022) 15:6811. doi: 10.3390/en15186811

49. Tan B, Cheng G, Zhu X, Yang X. Experimental study on the physisorption characteristics of O2 in coal powder are affected by coal nanopore structure. *Sci Rep*. (2020) 10:6946. doi: 10.1038/s41598-020-63988-4

50. Pushkar B, Sevak P, Parab S, Nilkanth N. Chromium pollution and its bioremediation mechanisms in bacteria: a review. *J Environ Manage*. (2021) 287:112279. doi: 10.1016/j.jenvman.2021.112279

51. Mistikawy JA, Mackowiak TJ, Butler MJ, Mischenko IC, Cernak RS, Richardson JB. Chromium, manganese, nickel, and cobalt mobility and bioavailability from mafic-to-ultramafic mine spoil weathering in western Massachusetts, USA. *Environ Geochem Health*. (2020) 42:3263–79. doi: 10.1007/s10653-020-00566-7

52. Wani KI, Naeem M, Aftab T. Chromium in plant-soil nexus: Speciation, uptake, transport and sustainable remediation techniques. *Environ pollut*. (2022) 315:120350. doi: 10.1016/j.envpol.2022.120350

53. Zulfiqar U, Haider FU, Ahmad M, Hussain S, Maqsood MF, Ishfaq M, et al. Chromium toxicity, speciation, and remediation strategies in soil-plant interface: A critical review. *Front Plant Sci*. (2023) 13:1081624. doi: 10.3389/fpls.2022.1081624

54. Kicińska A, Pomykała R, Izquierdo-Diaz M. Changes in soil pH and mobility of heavy metals in contaminated soils. *Eur J Soil Sci*. (2022) 73:01–14. doi: 10.1111/ejss.13203

55. Pierangeli MAP, Guilherme LRG, Oliveira LR, Curi N, Silva MLN. Efeito da força iônica da solução de equilíbrio sobre a adsorção/dessorção de chumbo em Latossolos brasileiros. *Pesq Agropec Bras*. (2001) 36:1077–84. doi: 10.1590/S0100-204X2001000800010

56. McBride MB. *Environmental chemistry of soils*. New York: Oxford University Press (1994). p. 406. 406pp.

57. Ward CR. Analysis, origin and significance of mineral matter in coal: An updated review. *Int J Coal Geol*. (2016) 165:1–27. doi: 10.1016/j.coal.2016.07.014

58. Cheng F, Zhang Y, Zhang G, Zhang K, Wu J, Zhang D. Eliminating environmental impact of coal mining wastes and coal processing by-products by high temperature oxy-fuel CFB combustion for clean power generation: A review. *Fuel*. (2024) 373:132341. doi: 10.1016/j.fuel.2024.132341

59. Li WW. Air pollution, air quality, vehicle emissions, and environmental regulations. In: *Traffic-related air pollution* (2020) Cambridge, MA, USA: Elsevier/Academic Press. p. 23–49. doi: 10.1016/B978-0-12-818122-5.00002-8

60. Zhang Y, Nie R, Shi R, Zhang M. Measuring the capacity utilization of the coal sector and its decoupling with economic growth in China's supply-side reform. *Resour Conserv Recy*. (2018) 129:314–25. doi: 10.1016/j.resconrec.2016.09.022

61. Dias SC. *Estudo pioneiro da restauração de solos minerados em uma cronosequência de 10,6 anos na mina de carvão de Moatize, Moçambique*., PhD dissertation. Pelotas, Brazil: Universidade Federal de Pelotas. (2024) 111. Available online at: https://guaiaca.ufpel.edu.br/handle/prefix/14559 (Accessed February 08, 2026).

62. Sanghaw R, Vityakon P, Rasche F. How feedback loops between meso- and macrofauna and organic residues contrasting in chemical quality determine decomposition dynamics in soils. *Heliyon*. (2023) 9:e15534. doi: 10.1016/j.heliyon.2023.e15534

63. Hoffland E, Kuyper TW, Comans RNJ, Creamer RE. Eco-functionality of organic matter in soils. *Plant Soil*. (2020) 455:1–22. doi: 10.1007/s11104-020-04651-9

64. Frouz J, Prach K, Pižl V, Háněl L, Starý J, Tajovský K, et al. Interactions between soil development, vegetation and soil fauna during spontaneous succession in post mining sites. *Eur J Soil Biol*. (2008) 44:109–21. doi: 10.1016/j.ejsobi.2007.09.002

65. Juan-Ovejero R, Álvarez-Rogel J, Peñalver-Alcalá A, Verweij RA, van Gestel CAM, González-Alcaraz MN. Microarthropod communities act as functional mediators of ecosystem recovery in abandoned metal(loid) mine tailings in semiarid areas. *Sci Total Environ*. (2023) 881:163394. doi: 10.1016/j.scitotenv.2023.163394

66. Chen C, Fang X, Xiang WH, Lei PF, Ouyang S, Kuzyakov Y. Soil-plant costimulation during forest vegetation restoration in a subtropical area of southern China. *For Ecosyst*. (2020) 7:1.17. doi: 10.1186/s40663-020-00242-3

67. Bai X, Guo Z, Huang Y, An S. Root cellulose drives soil fulvic acid carbon sequestration in the grassland restoration process. *Catena (Amst)*. (2020) 191:104575. doi: 10.1016/J.CATENA.2020.104575

68. Cui T, Zhang J, Luo W, Cui T, Zhang J, Luo W. The quantity and quality of humic substances following different land uses in Karst Peak-Cluster Depression in Guangxi, China. *Agriculture*. (2023) 13:2246. doi: 10.3390/AGRICULTURE13122246

69. Singh P, Ghosh AK. Ratio of elements in humic acids extracted from restored mine soil as a measure of quality of carbon sequestered. *Int J Chem Stud*. (2020) 8:1343–6. doi: 10.22271/CHEMI.2020.V8.I6S.10948

70. Raiesi F. The quantity and quality of soil organic matter and humic substances following dry-farming and subsequent restoration in an upland pasture. *Catena (Amst)*. (2021) 202:105249. doi: 10.1016/J.CATENA.2021.105249

71. De Feudis M, Falsone G, Vianello G, Antisari LV. Stable organic carbon pool rises in soil under chestnut (Castanea sativa Mill.) forest for timber production after 15 years since grafting onto satin-cut stumps. *EQA - Int J Environ Qual*. (2024) 40:1–10. doi: 10.6092/ISSN.2281-4485/10731

72. Seillier R, Paran F, Pauget B, Challaye C, Peuble S, Gallice F, et al. Rethinking soil contamination assessment for urban brownfield management: from total hazard to bioavailability. *Chemosphere*. (2025) 393:144769. doi: 10.1016/J.CHEMOSPHERE.2025.144769

73. Wang W, Xue J, Zhang L, He M, You J. Extraction of heavy metals from copper tailings by ryegrass (Lolium perenne L.) with the assistance of degradable chelating agents. *Sci Rep 2024 14:1*. (2024) 14:7663. doi: 10.1038/s41598-024-58486-w

74. Kim RY, Yoon JK, Kim TS, Yang JE, Owens G, Kim KR. Bioavailability of heavy metals in soils: definitions and practical implementation—a critical review. *Environ Geochemistry Health 2015 37:6*. (2015) 37:1041–61. doi: 10.1007/S10653-015-9695-Y

75. Yu Z, Liu E, Lin Q, Zhang E, Yang F, Wei C, et al. Comprehensive assessment of heavy metal pollution and ecological risk in lake sediment by combining total concentration and chemical partitioning. *Environ pollut*. (2021) 269:116212. doi: 10.1016/J.ENVPOL.2020.116212

76. Rincon-Vasquez IV, Fohrer N, Rosado D. Assessing sediment toxicity risks with bioavailable metal fractions: new factors and index applied to the Colombian tropical Andes hotspot. *Environ Geochemistry Health 2025 47:6*. (2025) 47:222. doi: 10.1007/S10653-025-02536-3

77. Jomova K, Alomar SY, Nepovimova E, Kuca K, Valko M. Heavy metals: toxicity and human health effects. *Arch Toxicol*. (2024) 99:153–209. doi: 10.1007/S00204-024-03903-2

78. Wang M, Song G, Zheng Z, Song Z, Mi X, Hua J. Effect of humic substances on the fraction of heavy metal and microbial response. *Sci Rep*. (2024) 14:11206. doi: 10.1038/s41598-024-61575-5